6.6 Hz, 2H, CH_3CH_2O), 5.21 (dd, ^3J(H,H) = 4.8, 8.4 Hz, 1H, C*H*–SePh), 7.19 – 7.64 (m, 10H, Ph), 8.05 (s, 1H, C*H*=C); ^{13}C NMR (100 MHz, $CDCl_3$): *Z* isomer: δ = 13.77, 14.17, 19.26, 31.17, 39.68, 60.62, 69.79, 85.91, 124.32, 127.46, 127.95, 128.77, 129.15, 133.24, 135.39, 147.51, 167.03; *E* isomer: δ = 12.93, 14.24, 19.29, 31.10, 41.69, 60.78, 69.72, 86.38, 127.39, 127.95, 128.54, 129.33, 132.93, 133.20, 135.26, 143.39, 164.79; IR (NaCl): $\tilde{\nu}$ = 1694 (C=O), 1574 cm^{-1} (C=C); MS (CI): *m*/*z* (%): 439 (7.0) [M^+ – BuO] or [M^+ – CO_2Et]; elemental analysis calcd for $C_{23}H_{28}O_3Se_2$: C 54.13, H 5.53; found: C 54.24, H 5.66.

Received: December 1, 1998 [Z 12734 IE]
German version: *Angew. Chem.* **1999**, *111*, 2066 – 2069

Keywords: alkenes · alkynes · C–C coupling · radical reactions · selenium

[1] U. Schmidt, A. Müller, K. Markau, *Chem. Ber.* **1964**, *97*, 405 – 414.
[2] PhS• is relatively reactive toward carbon – carbon double bonds compared with PhSe• [$k_{PhS•}/k_{PhSe•} = 10 – 50$]: O. Ito, *J. Am. Chem. Soc.* **1983**, *105*, 850 – 853, and references therein.
[3] $(PhSe)_2$ is more reactive toward alkyl radicals than $(PhS)_2$ [$k_{(PhSe)_2}/k_{(PhS)_2} \approx 160$]: a) G. A. Russell, H. Tashtoush, *J. Am. Chem. Soc.* **1983**, *105*, 1398 – 1399; b) M. J. Perkins, E. S. Turner, *J. Chem. Soc. Chem. Commun.* **1981**, 139 – 140; c) G. A. Russell, P. Ngoviwatchai, H. I. Tashtoush, A. Pla-Dalmau, R. K. Khanna, *J. Am. Chem. Soc.* **1988**, *110*, 3530 – 3538.
[4] For example, the photoinduced reaction of $(PhSe)_2$ with 1-hexene provided only 9% of the corresponding bis-selenide adduct on irradiation for 30 h: A. Ogawa, H. Tanaka, H. Yokoyama, R. Obayashi, K. Yokoyama, N. Sonoda, *J. Org. Chem.* **1992**, *57*, 111 – 115.
[5] a) A. Ogawa, H. Yokoyama, K. Yokoyama, T. Masawaki, N. Kambe, N. Sonoda, *J. Org. Chem.* **1991**, *56*, 5721 – 5723; b) T. G. Back, M. V. Krishna, *J. Org. Chem.* **1988**, *53*, 2533 – 2536; c) A. Ogawa, N. Takami, M. Sekiguchi, H. Yokoyama, H. Kuniyasu, I. Ryu, N. Sonoda, *Chem. Lett.* **1991**, 2241 – 2242.
[6] a) G. Stork, R. Mook, Jr., *Tetrahedron Lett.* **1986**, *27*, 4529 – 4532; b) G. Stork, R. Mook, Jr., *J. Am. Chem. Soc.* **1987**, *109*, 2829 – 2831; c) K. Nozaki, K. Oshima, K. Utimoto, *J. Am. Chem. Soc.* **1987**, *109*, 2547 – 2549; d) J. E. Brumwell, N. S. Simpkins, N. K. Terrett, *Tetrahedron* **1994**, *50*, 13533 – 13552; e) C. A. Broka, D. E. C. Reichert, *Tetrahedron Lett.* **1987**, *28*, 1503 – 1506; f) T. Kataoka, M. Yoshimatsu, Y. Noda, T. Sato, H. Shimizu, M. Hori, *J. Chem. Soc. Perkin Trans. 1* **1993**, 121 – 129.
[7] E. Lee, C. U. Hur, *Tetrahedron Lett.* **1991**, *32*, 5101 – 5102.
[8] In general, vinyl radicals are believed to be a mixture of stereoisomeric σ radicals, and a fast equilibrium is present between the stereoisomers: a) R. W. Fessenden, R. H. Schuler, *J. Chem. Phys.* **1963**, *39*, 2147 – 2195. In contrast, α-aryl-substituted vinylic radicals are assumed to be π radicals: b) L. A. Singer, J. Chen, *Tetrahedron Lett.* **1969**, 4849 – 4854.
[9] Ethyl propiolate is assumed to generate a vinylic π radical: a) C. Galli, A. Guarnieri, H. Koch, P. Mencarelli, Z. Rappoport, *J. Org. Chem.* **1997**, *62*, 4072 – 4077; b) H. Rubin, H. Fischer, *Helv. Chim. Acta* **1996**, *79*, 1670 – 1682; c) J. O. Metzger, M. Blumenstein, *Chem. Ber.* **1993**, *126*, 2493 – 2499.
[10] Although PhSe• can also add to alkenes, the reverse reaction from β-selenoalkyl radicals to give the starting alkenes and PhSe• is probably much faster than that of β-selenoalkenyl radicals to give the starting alkynes and PhSe•.
[11] a) M. Sevrin, D. Van Ende, A. Krief, *Tetrahedron Lett.* **1976**, 2643 – 2646; b) J. Lucchetti, A. Krief, *Tetrahedron Lett.* **1981**, *22*, 1623 – 1626; c) D. L. J. Clive, G. Chittattu, C. K. Wong, *J. Chem. Soc. Chem. Commun.* **1978**, 41 – 42; d) D. L. J. Clive, G. J. Chittattu, V. Farina, W. A. Kiel, S. M. Menchen, C. G. Russell, A. Singh, C. K. Wong, N. J. Curtis, *J. Am. Chem. Soc.* **1980**, *102*, 4438 – 4447; e) K. C. Nicolaou, *Tetrahedron* **1981**, *37*, 4097 – 4109; f) T. G. Back, *J. Chem. Soc. Chem. Commun.* **1984**, 1417 – 1418; g) C. Chatgilialoglu, M. Guerra, A. Guerrini, G. Seconi, K. B. Clark, D. Grillen, J. Kanabus-Kaminska, J. A. Martinho-Simões, *J. Org. Chem.* **1992**, *57*, 2427 – 2433.
[12] H. J. Reich, S. Wollowitz, *Org. React.* **1993**, *44*, 1 – 296, and references therein.
[13] J. V. Comasseto, *J. Organomet. Chem.* **1983**, *253*, 131 – 181.
[14] H. Okamura, M. Miura, K. Kosugi, H. Takei, *Tetrahedron Lett.* **1980**, *21*, 87 – 90.
[15] a) A. Ogawa, Y. Tsuboi, R. Obayashi, K. Yokoyama, I. Ryu, N. Sonoda, *J. Org. Chem.* **1994**, *59*, 1600 – 1601; b) J. V. Comasseto, L. W. Ling, N. Petragnani, H. A. Stefani, *Synthesis* **1997**, 373 – 403.
[16] The *E*/*Z* ratio of the product reflects that of the vinylic selenide starting material: **5b** *E*/*Z* = 10/90, **5j** *E*/*Z* = 7/93, **7b** *E*/*Z* = 7/93, **7b′** *E*/*Z* = 16/84, **7j** *E*/*Z* = 8/92.
[17] The relative rate of dichalcogenides for capturing carbon radicals is as follows: $k_{PhSSPh}:k_{PhSeSePh}:k_{PhTeTePh} = 1:160:630$.[3a]
[18] a) D. P. Curran in *Comprehensive Organic Synthesis*, *Vol. 4* (Eds.: B. M. Trost, I. Fleming, M. F. Semmelhock), Pergamon, Oxford, **1991**, pp. 779 – 831; b) D. P. Curran, *Synthesis* **1988**, 417 – 439; D. P. Curran, *Synthesis* **1988**, 489 – 513; c) D. P. Curran, N. A. Porter, B. Giese, *Stereochemistry of Radical Reactions*, VCH, Weinheim, **1996**; d) J. Fossey, D. Lefort, J. Sorba, *Free Radicals in Organic Chemistry*, Masson, Paris, **1995**; e) B. Giese, B. Kopping, T. Göbel, J. Dickhaut, G. Thoma, K. J. Kulicke, F. Trach, *Org. React.* **1996**, *48*, 301 – 856.

The First Determination of Eu–H Distances by Neutron Diffraction on the Novel Hydrides $EuMg_2H_6$ and $EuMgH_4$**

Holger Kohlmann,* Franz Gingl, Thomas Hansen, and Klaus Yvon

The complete crystal structure analysis of metal hydrides usually requires neutron diffraction data. Some elements, however, show excessively high absorption cross sections, σ_a, for neutrons, thus making this technique seemingly impractical. Natural europium (^{nat}Eu) consists of nearly equal amounts of the isotopes ^{151}Eu and ^{153}Eu. Its absorption cross section for thermal neutrons (σ_a = 4530 barns at λ = 179.8 pm) is higher than that of the shielding material cadmium.[1] Pure ^{153}Eu has a lower σ_a but is extremely expensive. Thus no complete, refined crystal structure data are known for europium hydrides, that is no reliable value exists for the distance Eu–H.[2]

Fortunately, the neutron absorption cross section of natural europium is strongly wavelength dependent and shows a minimum at λ = 72 pm (Figure 1). This prompted us to perform the first neutron diffraction experiment at this

[*] Dr. H. Kohlmann, Dr. F. Gingl,[+] Prof. Dr. K. Yvon
Laboratoire de Cristallographie
Université de Genève
Quai Ernest Ansermet 24, CH-1211 Genève 4 (Switzerland)
Fax: (+41) 22-7026108
E-mail: Holger.Kohlmann@cryst.unige.ch
Dr. T. Hansen
Institut Laue-Langevin, Grenoble (France)
[+] Current address:
National Institute of Materials and Chemical Research,
Tsukuba (Japan)

[**] We thank Dr. P. Fischer and M. Koch, Paul-Scherrer-Institut, Villigen (Switzerland) for helpful discussions and for providing a sample holder for neutron diffraction, and Dr. B. Revaz, Université de Genève (Switzerland), for the magnetic susceptibility measurement. This work was supported by the Swiss National Science Foundation and the Swiss Federal Office of Energy.

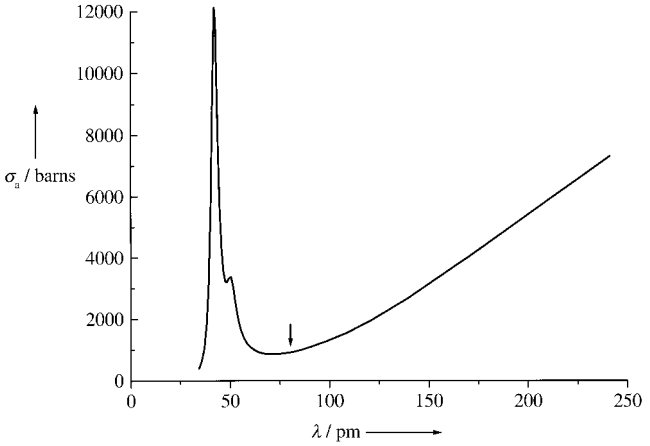

Figure 1. The absorption cross section of natural europium for neutrons as a function of the wavelength, calculated from $\sigma_a = 4\pi/k\, b_c''$ (k = norm of the neutron radiation wave vector; $b\ b_c''$ = imaginary part of the coherent scattering length according to Lynn[3]). The wavelength used for the neutron diffraction experiment ($\lambda = 80.45$ pm) is marked by an arrow.

wavelength on ^{nat}Eu-containing hydrides. The intensively colored carmine-red $EuMg_2H_6$ and brown $EuMgH_4$, which are the first ternary hydrides known in the Eu-Mg-H system, appeared to be well suited for this purpose (see Experimental Section). Since single crystals were not available, the structures were solved from powder diffraction data. The X-ray pattern of $EuMg_2H_6$ was indexed to a tetragonal unit cell[4] and the $EuMg_2$ substructure solved ab initio. The patterns of $EuMgH_4$ suggested an isotypic structure to orthorhombic $SrMgH_4$ (noncentrosymmetric) or $BaMgH_4$ (centrosymmetric),[4, 5] but did not allow to differentiate between these two models. Neutron diffraction data of two deuterated, multiphase samples were collected on the diffractometer D20 equipped with a position-sensitive detector at the high-flux reactor at the Insitut Laue-Langevin (Grenoble) at $\lambda = 80.45$ pm (Figure 2). All deuterium positions could be located and refined. Owing to its higher transmission the $EuMg_2D_6$ sample yielded more precise data than the $EuMgD_4$ sample (calculated: $T = e^{-\mu x} = 0.45$ and 0.08; Tables 1 and 2).

$EuMg_2H_6$ crystallizes in a novel AB_2X_6 type structure which can be described either as a stuffed variant of the ReO_3 type (BX_3), or as an ordered vacancy variant of the cubic perovskite type (ABX_3). Hydrogen occupies the X, magnesium the B, and europium half of the A sites. Its structural relationship to the cubic perovskite type can be illustrated by means of group–subgroup relationships (Figures 3a and 4). The doubling of the c axis in the second step of the symmetry reduction causes a splitting of the A cation position in two symmetry-independent sites, from which only one is occupied by europium. The niobium and tantalum bronzes AB_3O_9 ($= A_{2/3}B_2O_6$; A = La–Nd; B = Nb, Ta) and ANb_4O_{12} ($= A_{1/2}Nb_2O_6$; A = Th, U)[9] can be described as defect variants of the $EuMg_2H_6$ type, which are orthorhombically distorted for B = Nb.

Europium has a nearly cuboctahedral, and magnesium a nearly octahedral deuterium configuration in $EuMg_2D_6$. The metal coordination of deuterium is quadratic-bipyramidal

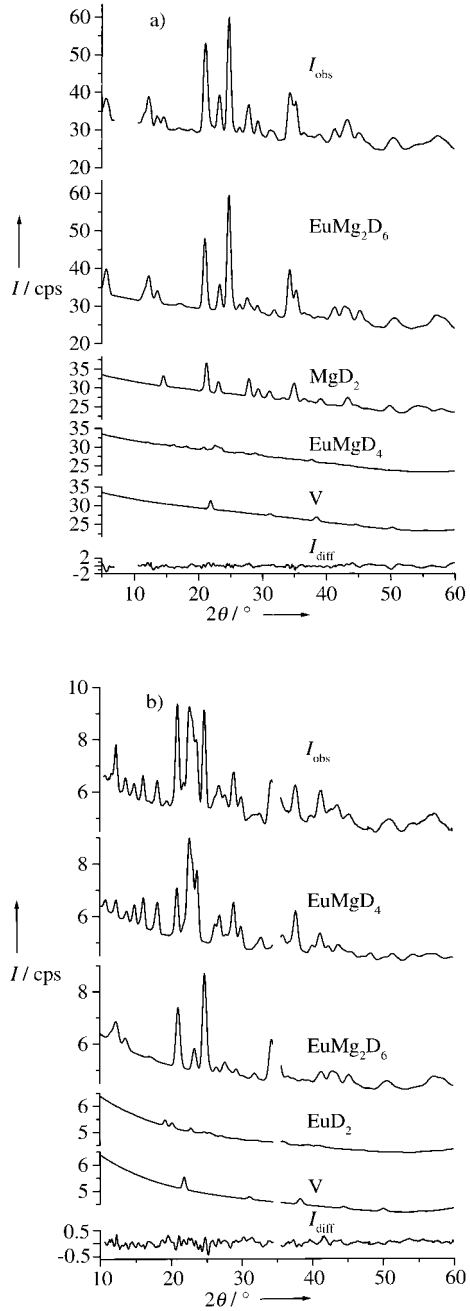

Figure 2. Graphical representation of the Rietveld refinement of the crystal structures of $EuMg_2D_6$ and $EuMgD_4$. From top to bottom: a, b) observed neutron diffraction pattern of the $EuMg_2D_6$ sample and of the $EuMgD_4$ sample, respectively, calculated patterns of $EuMg_2D_6$ and of $EuMgD_4$, respectively, of the by-products MgD_2 and $EuMgD_4$ and $EuMg_2D_6$ and EuD_2, respectively, as well as of vanadium (sample holder) and the difference pattern. Intensity in counts per second; refinement using the program FULLPROF,[6] neglecting the angular dependence of the absorption ((a) ca. 5%, (b) ca. 30%). Data collection: diffractometer D20, Institut Laue-Langevin, Grenoble (France); $\lambda = 80.45$ pm; $T = 293$ K; calculated linear absorption coefficients $\mu = 8.09$ cm^{-1} (a), $\mu = 12.53$ cm^{-1} (b); 1.5 g each in double-walled vanadium cylinder with $d_i = 13.5$ mm (a), 7 mm (b); $d_o = 14.5$ mm (a), 9 mm (b); data collection time 7 h (a), 13.5 h (b); 515 (a), 485 data points (b); blanks correspond to excluded regions due to detector failure.

(D2: 4 Eu + 2 Mg), saddlelike (D1: 2 Eu + 2 Mg) or linear (D3: 2 Mg). The latter geometry is remarkable insofar as linear Mg-H-Mg units have never been observed in saltlike hydrides.

  1433-7851/99/3813-2030 $ 17.50+.50/0 *Angew. Chem. Int. Ed.* **1999**, *38*, No. 13/14

Table 1. Crystal structure data of $EuMg_2D_6$ refined from neutron powder diffraction data (*P4/mmm*, $a = 376.57(5)$, $c = 799.2(2)$ pm, $T = 293$ K, $R_p = 0.075$, $R_{wp} = 0.063$, $R_{Bragg} = 0.039$). Temperature factor $T = \exp(-B_{iso}(\sin\theta/\lambda)^2)$.

Atom	Site	Symmetry	*x/a*	*y/b*	*z/c*	B_{iso} [10^4 pm^2]
Eu	1*a*	4/*mmm*	0	0	0	1.3(1)
Mg	2*h*	4*mm*	$\frac{1}{2}$	$\frac{1}{2}$	0.2779(8)	0.05(9)
D1	4*i*	2*mm*.	0	$\frac{1}{2}$	0.2132(4)	1.80(7)
D2	1*c*	4/*mmm*	$\frac{1}{2}$	$\frac{1}{2}$	0	B_{iso}(D1)
D3	1*d*	4/*mmm*	$\frac{1}{2}$	$\frac{1}{2}$	$\frac{1}{2}$	B_{iso}(D1)

Table 2. Crystal structure data of $EuMgD_4$ refined from neutron powder diffraction data ($Cmc2_1$, $a = 392.97(5)$,[a] $b = 1346.8(2)$,[a] $c = 553.86(7)$ pm,[a] $T = 293$ K, $R_p = 0.096$, $R_{wp} = 0.078$, $R_{Bragg} = 0.069$). Temperature factor as in Table 1.

Atom	Site	Symmetry	*x/a*	*y/b*	*z/c*	B_{iso} [10^4 pm^2]
Eu	4*a*	*m*..	0	0.1523(4)[a]	0.25(–)	2.5(4)
Mg	4*a*	*m*..	0	0.405(2)	0.193(5)	3.9(5)
D1	4*a*	*m*..	0	0.332(2)	0.464(5)	2.3(2)
D2	4*a*	*m*..	0	0.292(2)	0.990(5)	B_{iso}(D1)
D3	4*a*	*m*..	0	0.069(2)	0.662(3)	B_{iso}(D1)
D4	4*a*	*m*..	0	0.540(2)	0.342(3)	B_{iso}(D1)

[a] Refined from X-ray powder diffraction data, fixed in the refinement on the neutron data.

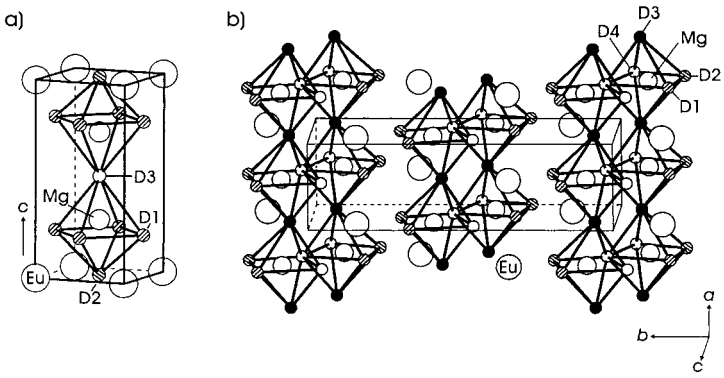

Figure 3. Crystal structure of a) $EuMg_2D_6$ (distances [pm]: Eu–8D1 253.9(2), Eu–4D2 266.21(1), Mg–D3 177.4(7), Mg–4D1 195.2(2), Mg–D2 222.0(7))[7] and b) $EuMgD_4$ (distances [pm] Eu–D2 237(2), Eu–2D2 249(2), Eu–2D1 253(2), Eu–2D4 254(1), Eu–D3 254(3), Eu–D1 270(2), Mg–D1 179(4), Mg–D2 189(4), Mg–D4 199(4), Mg–2D3 200.3(8), Mg–D4 208(3)).

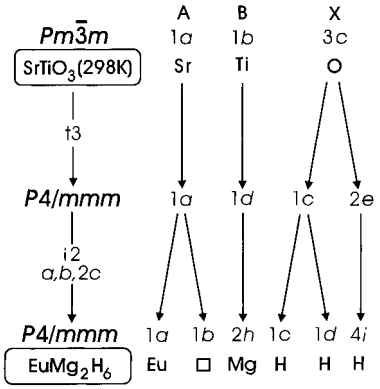

Figure 4. Crystallographic group–subgroup relationships according to Bärnighausen[8] between the crystal structure types of cubic perovskite $SrTiO_3$ and $EuMg_2H_6$

Hence, the Mg–D3 distance is very short (177 pm), the shortest ever reported in magnesium-containing metal hydrides. The shortest D–D contacts are 253.9(2) pm.

$EuMgH_4$ (Figure 3b) crystallizes in the orthorhombic $BaZnF_4$ type (space group $Cmc2_1$) and has similar atomic parameters to $SrMgH_4$.[5a] The EuMg sublattice displays a pseudo-symmetry which is the reason why the X-ray data could be well modeled with the centrosymmetric $BaMgH_4$ structure (space group *Cmcm*).[5b] Europium is surrounded by nine deuterium atoms in a distorted tricapped trigonal-prismatic configuration, and magnesium has a distorted octahedral deuterium coordination. As in $EuMg_2D_6$ the MgD_6 octahedra are linked through common corners. However, unlike $EuMg_2D_6$ in which the MgD_6 octahedra form a three-dimensional network, the octahedra in $EuMgD_4$ are linked in two directions only, thus forming two-dimensional layers in accordance with the higher D:Mg ratio (Figure 3). Deuterium is threefold (D3) and fourfold (D1, D2, D4) coordinated by metal atoms. The shortest D–D distance is 241(3) pm.

Studies of the magnetism (Figure 5) indicated ferromagnetic order for both compounds. The ordering temperatures T_C as extrapolated from the linear part of the plots of χ^{-1} versus T are 27 K for $EuMg_2D_6$ and 19 K for $EuMgD_4$. The

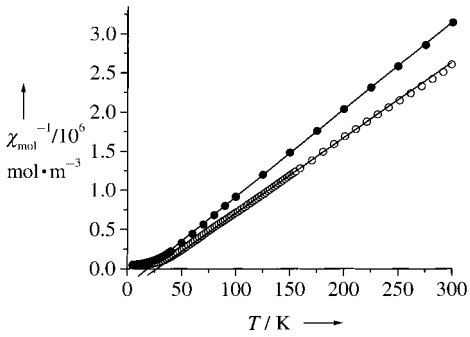

Figure 5. The reciprocal molar magnetic susceptibility of $EuMg_2D_6$ (open circles) and $EuMgD_4$ (filled circles) as a function of temperature (SQUID magnetometer, powder pellets, $B = 2$ T). The content of by-products ($EuMgD_4$ in the $EuMg_2D_6$ sample and vice versa) was estimated from a phase analysis by X-ray diffraction and considered in the calculation of magnetic moments. The fit of the linear part leads to the values $T_C = 27.2(5)$ K, $\mu_{eff} = 8.12(2)\,\mu_B$ for $EuMg_2D_6$, and $T_C = 18.7(5)$ K, $\mu_{eff} = 7.54(2)\,\mu_B$ for $EuMgD_4$.

calculated magnetic moments (8.1 and 7.5 μ_B) confirm the presence of Eu^{II} (theoretical values for free ions: 7.95 μ_B for Eu^{2+}, 0 μ_B for Eu^{3+}). The deviations from the theoretical value might be explained by crystal field effects and the presence of impurities. Thus $EuMg_2H_6$ and $EuMgH_4$ can be considered as nonmetallic, ionic solids, which is consistent with their red and brown colors, respectively.

Divalent lanthanides such as Eu^{II} and Yb^{II} can usually be substituted in solid-state compounds by alkaline earth elements such as Sr and Ca, respectively. This is particularly true for metal hydrides. All Eu- and Yb-containing hydrides known crystallize with structures isotypic to their Sr and Ca analogues, respectively. The $EuMgH_4/SrMgH_4$ pair is a further example. $EuMg_2H_6$, however, appears to be an exception as

no Sr analogue is known. Hydrogenation of $SrMg_2$ yields the phase $Sr_2Mg_3H_{10}$[10] to which no corresponding compound in the Eu-Mg-H system could be found (see Experimental Section).

The structure data of $EuMg_2D_6$ and $EuMgD_4$ provide the first refined Eu–D distances. The values for the various coordination numbers are 266 (Eu[12]-D[6]), 254 (Eu[12]-D[4]), and 252 pm (Eu[9]-D[4]). The collection of these data became possible through the development of advanced neutron diffractometers and detectors with a high flux neutron source. This underlines the importance of instrumental developments on such sources for solid-state research.

Experimental Section

$EuMg_2$ and EuMg, prepared by arc-melting of the elements (Eu 99.9 %, Mg 99.95 %) at the nominal composition 1:3 and 1:1.3, respectively, were hydrogenated (deuterated) in an autoclave at 600 K and 50 bar $H(D)_2$ pressure. The excess of Mg compensated the sublimation losses in the arc furnace. Owing to their moisture sensitivity $EuMg_2H_6$ and $EuMgH_4$ were handled in an argon-filled glove box. Both hydrides decompose at 800 K and 5 bar H_2 pressure into EuH_2 and Mg metal. Variations of the sample composition and synthesis conditions gave no evidence for the existence of further ternary phases in the Eu-Mg-H system.

Received: February 4, 1999 [Z12995IE]
German version: *Angew. Chem.* **1999**, *111*, 2145 – 2147

Keywords: europium · metal hydrides · neutron absorption · neutron diffraction · structure elucidation

[1] V. F. Sears, *Neutron News* **1992**, *3*, 26 – 37.
[2] Neutron diffraction has been used so far only for $^{153}Eu_2IrD_5$, but no structure refinement was performed: J. Zhuang, W. Kunnmann, L. M. Corliss, J. M. Hastings, R. O. Moyer, Jr., *J. Solid State Chem.* **1983**, *48*, 117 – 120.
[3] J. E. Lynn, *J. Appl. Crystallogr.* **1989**, *22*, 476 – 482.
[4] X-ray diffraction: $EuMg_2H_6$: $a = 377.17(2)$, $c = 799.44(7)$ pm; $EuMgH_4$: $a = 392.79(8)$, $b = 1346.3(2)$, $c = 555.2(1)$ pm ($T = 293$ K); no phase transition down to $T = 12$ K.
[5] a) F. Gingl, K. Yvon, P. Fischer, *J. Alloys Compd.* **1992**, *187*, 105 – 111; b) F. Gingl, K. Yvon, T. Vogt, *J. Alloys Compd.* **1997**, *256*, 155 – 158.
[6] J. Rodriguez-Carvajal, FULLPROF, Version 3.2, **1997**.
[7] Calculated by using lattice parameters from X-ray data ($a = 376.48(2)$, $c = 798.84(6)$ pm, $T = 293$ K; Table 1).
[8] H. Bärnighausen, *MATCH* **1980**, *9*, 139 – 175.
[9] a) A. M. Abakumov, R. V. Shpanchenko, E. V. Antipov, *Mat. Res. Bull.* **1995**, *30*, 97 – 103; b) P. N. Iyer, A. J. Smith, *Acta Crystallogr.* **1967**, *23*, 740 – 746; c) A. Ibarra-Palos, M. E. Villafuerte-Castrejón, J. Duque, R. Pomés, *J. Solid State Chem.* **1996**, *124*, 272 – 277; d) M. A. Alario-Franco, I. E. Grey, J. C. Joubert, H. Vincent, M. Labeau, *Acta Crystallogr. Sect. A* **1982**, *38*, 177 – 186; e) M. Labeau, I. E. Grey, J. C. Joubert, J. Chenevas, A. Collomb, J. C. Guitel, *Acta Crystallogr. Sect. B* **1985**, *41*, 33 – 41.
[10] F. Gingl, K. Yvon, P. Fischer, *J. Alloys Compd.* **1994**, *206*, 73 – 75.

Design, Synthesis, and Evaluation of Novel Modular Bisubstrate Analogue Inhibitors of Farnesyltransferase**

Martin Schlitzer* and Isabel Sattler

The ras signal transduction pathway plays a decisive role in cell growth and differentiation. Point mutations in the *ras* gene can lead to *ras* proteins of constitutive activity, that is, they are unable to return to an inactive form after activation. These mutant variants deliver constant signals to the nucleus, which result in growth stimulation. Such ras mutations have been found in nearly 30 % of all tumors; the incidence can be as high as 90 % in certain tumor types.[1] Ras proteins must be post-translationally modified for localization at the inner cell membrane. The first such modification, crucial to the function of both normal and mutant ras proteins, is catalyzed by farnesyltransferase (FTase), which transfers a farnesyl residue from farnesylpyrophosphate (FPP) to the side chain SH group of cysteine in the C-terminal sequence CAAX (C: cysteine, A: aliphatic amino acid, X: C-terminal methionine or serine).[1] Both FPP and the CAAX tetrapeptide serve as suitable templates for FTase inhibitors. Bisubstrate analogue inhibitors, which contain elements from both peptide and farnesyl moieties, represent a further class of FTase inhibitors.[1a, 2] Such bisubstrate inhibitors are of particular interest as they can circumvent the need for the free SH function present in almost all CAAX peptidomimetics.[3] Such free SH groups are unfavorable both as a result of their inherent chemical sensitivity and, more importantly, because they are a source of serious side effects as seen, for example, with the antihypertensive drug Captopril.[4] In addition, recent kinetic studies show that FTase has an unusually high affinity for its product, the farnesylated ras protein, which is only released upon binding of a further FPP molecule.[5]

Bisubstrate inhibitors, which represent product analogues, should therefore be particularly good FTase inhibitors.[5] Few bisubstrate or product analogues have been reported to date. Recently, Waldmann et al. synthesized the natural product pepticinnamin E (**1**, Scheme 1) in multiple step reaction sequence and showed it to be a suitable model for bisubstrate FTase inhibitors.[6]

Herein we present a novel class of fully synthetic modular bisubstrate inhibitors. Our aim was to develop a bisubstrate inhibitor containing a peptidomimetic (corresponding to CAAX) and a non-prenyl lipophilic group (corresponding to farnesyl). In a series of *N*-acylaspartates, for example, **2** (Scheme 1) we have identified the benzyloxycinnamoyl moiety as a suitable farnesyl mimetic.[7] The FPP analogue,

[*] Dr. M. Schlitzer
Institut für Pharmazeutische Chemie der Universität
Marbacher Weg 6, D-35032 Marburg (Germany)
E-mail: schlitze@mailer.uni-marburg.de
Dr. I. Sattler
Hans-Knöll-Institut für Naturstoff-Forschung e.V., Jena (Germany)

[**] We are grateful to Prof. Tamanoi (UCLA) for the plasmids pGEX-DPR1 and pBC-RAM2, Dr. M. T. Stubbs for translating the manuscript, and to Prof. Dr. W. Hanefeld (Marburg), Prof. Dr. S. Grabley (Jena), and Dr. R. Thiericke (Jena) for their generous support.

  1433-7851/99/3813-2032 $ 17.50+.50/0